A Study on the Temperature of Ohmic Contact to p-Type SiC Based on Ti 3 SiC 2 Phase

Tony Abi-Tannous, Maher Soueidan, Gabriel Ferro, Mihai Lazar, Christophe Raynaud, Berangere Toury, Marie-France Beaufort, Jean François Barbot, Olivier Dezellus, Dominique Planson

A study in temperature of ohmic contact on p-type SiC based on Ti_3SiC_2 phase

Tony Abi-Tannous, Maher Soueidan, Gabriel Ferro, Mihai Lazar, Christophe Raynaud, Bérangère Toury, Marie-France Beaufort, Jean-Francois Barbot, Olivier Dezellus, and Dominique Planson

Abstract— **In this paper, the electrical properties of Ti_3SiC_2 based ohmic contacts formed on p-type 4H-SiC were studied. The growth of Ti_3SiC_2 thin films were studied onto 4H-SiC substrates by thermal annealing of Ti-Al layers deposited by magnetron sputtering. In this study, we varied the concentration of Ti and Al ($Ti_{20}Al_{80}$, $Ti_{30}Al_{70}$, $Ti_{50}Al_{50}$ and Ti), and the annealing temperature from 900°C to 1200°C for each concentration. X-Ray Diffraction and Transmission Electron Microscopy analyzes were performed on the samples to determine the microstructure of the annealed layers and to further investigate the compounds formed after annealing. Using TLM structures, the Specific Contact Resistance (SCR) at room temperature of all contacts was measured. The temperature dependence up to 600°C of the SCR of the best contacts was studied to understand the current mechanisms at the Ti_3SiC_2/SiC interface. Experimental results are in agreement with the thermionic field emission (TFE) theory. With this model, the barrier height of the contact varies between 0.71 to 0.85 eV. Finally, ageing tests showed that Ti_3SiC_2 based contacts were stable and relabel up to 400 h at 600°C under Ar.**

Index Terms— **Ohmic contact, silicon carbide, Ti-Al alloy, Ti_3SiC_2, TFE**

I. Introduction

Due to its wide bandgap, high electric field strength and high thermal conductivity, but also to its technological maturity, Silicon Carbide (SiC) is the most likely of all the wide band-gap semiconductors to succeed Silicon (Si) for high power density and high temperature device applications [1-4]. But, the high-temperature functionality of SiC devices is useless without ohmic contacts that are also able to operate under the same conditions. The stability of metal–semiconductor contacts is one of the factors which limit the high-temperature operation of SiC electronic devices and circuits. This is generally associated with the evolution of the nature and/or structure of the metal–
SiC interface through continuing reactions forming silicides, carbides, free carbon, and/or oxides. Further complications are introduced by the requirements for high temperature ohmic contacts such as i) high resistance to oxidation, ii) stable electrical conductivity and contact resistance, iii) low resistivity, iv) the ability to be connected to external circuitry and v) the reliability at high temperature.

P-type 4H-SiC has a high work function (~7 eV) and it's difficult to found a conventional metal that leads to low Schottky barrier height (SBH) when deposited on p-type 4H-SiC [5]. Such contacts are generally employed containing aluminium [6], and while many different alloys have been investigated, a great deal of attention has been focused on Al-Ti [5, 7, 8, 9, 10], which has demonstrated specific contact resistances on the order of 10^{-3}–10^{-5} $\Omega.cm^2$ on p-type SiC. Other investigations have focused on Ni/Ti/Al contact fabricated on highly p-type 4H-SiC [11] leading to low specific contact resistance (2.8×10^{-6} $\Omega.cm^2$), but this result was not reproducible.

To date, Al-Ti alloy remains the only material that has been shown to result in stable low-resistance ohmic contacts to p-type SiC due to the formation of Ti_3SiC_2 after annealing at high temperature [5, 12, 13]. Ti_3SiC_2 is layered ternary carbide which belongs to the $M_{n+1}AX_n$ (MAX) compounds [14, 15]. It is thought to be one of the best candidate materials for high temperature ohmic contact issues to SiC because of the following reasons : i) it advantageously combines metallic and ceramic properties, ii) has good thermal and electrical conductivity (37 $Wm^{-1}.K^{-1}$ and 4.6×10^6 $\Omega^{-1}m^{-1}$ respectively), iii) has relatively low thermal expansion coefficients (8.10^{-6} /°C) which value is closed to SiC (4.10^{-6} /°C), iv) is a very stable compound in air up to 1400°C and v) Ti_3SiC_2 and SiC are in thermodynamic equilibrium so that the interface should remain stable even at high temperature (higher than 1200 °C) [16, 17].

This paper reports on the electrical characterization of Ti-Al ohmic contact to p-type 4H-SiC. We study the effect of Ti-Al composition and annealing temperature for the formation of ohmic contact, which can be used in various electronic devices (bipolar diodes, BJT, Thyristors, JFET…). Finally, the temperature dependence of the electrical properties up to 600°C **and after 400 h of ageing at 600°C are discussed.**

II. Experimental section

A. Sample Preparation

P-type epilayers (~1.3 µm thick) doped with Al in the [1-4] $\times10^{19}$ cm^{-3} range on 4H-SiC (0001) 4°off substrates were used in this study. The samples are chemically cleaned to remove any surface pollution. This implies acetone and ethanol ultrasonic degreasing for 5 min each, followed by two times H_2SO_4: H_2O_2 (2: 1) for 10 minutes and finally HF acid

T.Abi-Tannous, M. Soueidan, M. Lazar, C. Raynaud and D. Planson are with Lyon University, CNRS, Ampère laboratory, INSA-Lyon, UMR 5005, F-69621, France.

G. Ferro, B. Toury and O. Dezellus are with Lyon University, CNRS, Laboratoire des Multimatériaux et Interfaces, UMR 5615, F-69622, France.

M.F. Beaufort and J.F. Barbot are with Poitiers University, CNRS, Pprime Institut, ENSMA - UPR 3346, SP2MI-86962, France.

diluted at 5% for 4 min, before rinsing with deionized water and blown dry in N_2 gas. The tested SiC layer was isolated by RIE etching forming mesa structures. The SiC etching was performed in an Alcatel Nextral NE110 reactor during 7 min, with a pressure of 60 mTorr and a power (RF) of 250 W. The reactive gas is composed by SF_6 (25 sccm) and O_2 (7 sccm). After RIE, the samples underwent a second chemical cleaning as mentioned above. And then two sets of samples were prepared on such substrates:

(1) **Ti-Al stacking**: 200 nm of Ti_xAl_{100-x} ($20\ at\% \leq x \leq 50\ at\%$) deposited by magnetron sputtering from Ti_xAl_{100-x} target in a high vacuum system. The deposition was carried out at room temperature with an Ar constant pressure (5×10^{-3} mbar).

(2) **Pure Ti**: 200 nm of pure Ti was deposited using e-beam evaporator in a high vacuum chamber.

After metal deposition, Transfer Length Method (TLM) structures were fabricated on the mesa in order to characterize electrically the metal/SiC p-type contact. The geometric patterns for the TLM measurements were obtained through a photolithographic procedure. The unwanted metal was removed by wet etching using commercial Al-etch at 60°C. The TLM contact consists of seven rectangular electrodes ($500 \times 100\ \mu m^2$) with increasing spacing of 3, 6, 10, 20, 40, 80 and 120 µm. For ohmic contact formation, high temperature annealing was performed in a Rapid Thermal Annealing (RTA) furnace under argon at atmospheric pressure with advanced backing steps (3 times pumping followed by argon filling) before the annealing in order to decrease the residual oxygen concentration in the RTA chamber. The beneficial effect of such baking steps is described in references [18, 19]. The annealing temperature was varied from 900 to 1200°C for 10 min plateau and a heating rate of 20°C/s. After annealing, the dimensions of the TLM patterns and the interpad distances remained unchanged. This was confirmed by measurements using optical microscope. So, no correction has been performed during the TLM measurements. Note that the "current crowding effect" is negligible since the length of the rectangular pads (500 µm) is very big compared to the distance between the pads and the distance between the pads and the edge of the mesa (5 µm).

B. Sample characterizations

The structural characterizations were mainly performed using X-Ray Diffraction (XRD), and Transmission Electron Microscopy (TEM). The XRD measurements were conducted on a D8 BRUKER with Cu K_α radiation. The Cross-sectional TEM (XTEM) samples were thinned down to 10 µm by using the tripod polisher. The electron transparency was achieved by ion milling.

For electrical characterization the samples are mounted directly on the heating chuck of a probe station. The samples are characterized up to 600°C and the temperature is monitored using a K-Type thermocouple. Our tests showed a temperature accuracy value of ±1%. Above 300°C, tests are performed under vacuum to prevent oxidation of the TLM structures. The electrical measurements are performed using a Keithley Source Measurement Unit K2602A. A four-probes setup is used (Kelvin configuration) to eliminate cable and tips resistances, which results in a measurement accuracy value better than 1%. I-V characteristics are plotted as function of the contact spacing of different temperatures.

III. Results and discussion

A. Identification of reaction products

TABLE I lists the reaction products obtained by XRD for all samples ($Ti_{20}Al_{80}$, $Ti_{30}Al_{70}$, $Ti_{50}Al_{50}$ and Ti) after annealing at various temperatures. From the Ti_3SiC_2 peaks all belonging to the (0 0 L) family (L = from 2 to 12), we can deduce that the Ti_3SiC_2 material formed has an epitaxial relationship with the SiC substrate. Epitaxial Ti_3SiC_2 on SiC, obtained by Ti-Al annealing, was already reported by Parisini and al. [20] and Tsukimoto and al. [21].

Transmission Electron Microscopy (TEM) investigations were carried on $Ti_{30}Al_{70}$ annealed at 1000°C and Ti annealed at 1200°C. Fig. 1-a displays a bright field (BF) filtered image of a typical region of the as-obtained layer on 4H-SiC from $Ti_{30}Al_{70}$ annealed at 1000°C. This general view shows that the 4H-SiC substrate is entirely covered by a Ti_3SiC_2 layer, which is itself covered by an Al rich layer. On the other hand, for Ti annealed at 1200°C (Fig. 1-b), the 4H-SiC substrate is again entirely covered by a Ti_3SiC_2 layer, but there is a strongly modified SiC region on the side of the interface coming from the solid-solid reaction between Ti and SiC. When comparing with the results obtained using Al based contacts, Al play the role of liquid phase promoter, leading to a less damaged interface. For more details about the interfacial reaction check ref. [18].

B. Electrical characterization at room temperature

Using TLM structures, the electrical characterization of the contact resistance was performed by means of current-voltage (*I-V*) measurements. Fig. 2 shows the corresponding room-temperature I–V characteristics measured between two adjacent TLM pads taken from $Ti_{50}Al_{50}$ contacts, as-deposited and after thermal annealing at 900, 1000, 1100, 1200°C.

A non-ohmic behavior was observed on as-prepared samples and on samples annealed at 900°C. But for the samples annealed at 1000°C or above, I-V behaviors are linear and prove that the contact is ohmic.

TABLE I
THE REACTION PRODUCTS IDENTIFIED BY XRD, FOR ALL SAMPLES AFTER ANNEALING AT 900, 1000, 1100, 1200°C. **(*)**: SMALL PEAKS, **(§)**: SMALL AND SHIFTED PEAKS.

	900°C	1000°C	1100°C	1200°C
$Ti_{20}Al_{80}$	Ti_3SiC_2 Al_4C_3 - Al Al_3Ti	Ti_3SiC_2**(*)** TiC - Al_4C_3 Al - Al_3Ti	TiC - Al_4C_3 Al - Al_3Ti	TiC - Al_4C_3 Al - Al_3Ti
$Ti_{30}Al_{70}$	Ti_3SiC_2 - Al Al_3Ti	Ti_3SiC_2 - Al Al_3Ti	Ti_3SiC_2**(*)** TiC - Al	Ti_3SiC_2**(*)** TiC - Al
$Ti_{50}Al_{50}$	Ti_3SiC_2 **(§)**	Ti_3SiC_2 Al – Al_3Ti	Ti_3SiC_2 - Al	Ti_3SiC_2 -Al Al_3Ti
Ti	Ti_3SiC_2 **(*)** TiC	Ti_3SiC_2 **(*)** TiC	Ti_3SiC_2 TiC	Ti_3SiC_2 TiC

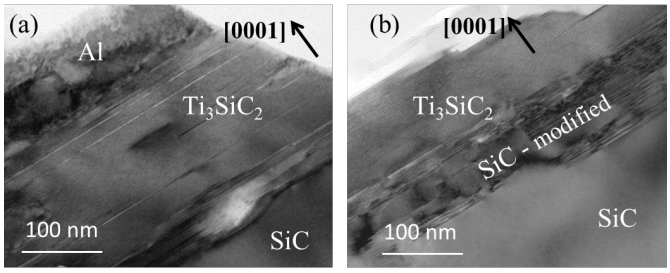

Fig.1. XTEM-BF image taken along the [11–20] SiC zone axis showing that (a) after annealing of $Ti_{30}Al_{70}$ at 1000°C, Ti_3SiC_2 covers completely the surface of the SiC and is itself covered by an Al layer. And (b) after annealing of Ti at 1200 °C, modified SiC covers the surface of the SiC and is itself covered by a Ti_3SiC_2 layer

Fig. 3 shows a typical set of curves obtained from TLM measurements from those contacts (i.e. $Ti_{50}Al_{50}$ annealed at 1000, 1100 or 1200°C) that displayed ohmic characteristics for the purpose of extracting the Specific Contact Resistance (SCR) ρ_c. As seen, the TLM plots have a different slope at different annealing temperatures; it means that the sheet resistance of the p-layer is different between the samples. This is due to the fact that the annealing was achieved on different samples having a doping concentration varied between 1 and 4 $\times 10^{19}$ cm^{-3}. The $Ti_{50}Al_{50}$ annealed at 1000°C yielded the lowest SCR of 1.1 $\times 10^{-4}$ $\Omega.cm^2$ (and also the lowest R_{on}). This SCR increases with increasing annealing temperature as can be seen from TABLE II and Fig. 4. From this Table and Figure, one can also follow the electrical properties of the others types of contacts ($Ti_{30}Al_{70}$, $Ti_{20}Al_{80}$ and Ti) annealed at different temperatures and evaluated by TLM analysis at room temperature. As can be seen, the trends are rather similar for these contacts except for the case of pure Ti for which a non-ohmic behavior was always observed. This is probably due to the modified SiC region at the interface.

However, when we add Al, the electrical behavior of the contact become ohmic and ρ_c increases when the Al content increases. That means the addition of Al to the Ti is necessary for the formation of ohmic contact with low resistivity. The main reason for this variation is still unknown and more physical and chemical characterizations to the interface should be done in order to elucidate this behavior. Moreover, for all compositions containing Al, the ρ_c increases when the annealing temperature increases from 1000 to 1200°C and this is probably due to the formation of TiC with Ti_3SiC_2.

We note in spite of a high roughness observed on our contacts (~45nm root mean squared, measured by Atomic Force Microscopy), excellent edge acuity is obtained. This is independent on the Al concentration, on all TLM pads and we carefully measured the width and the distances between the TLM pads.

According to the results presented in Fig. 4 and TABLE II, the samples annealed at 1000°C resulted in the lowest contact resistivities and hence were selected for further electrical measurements at high temperature.

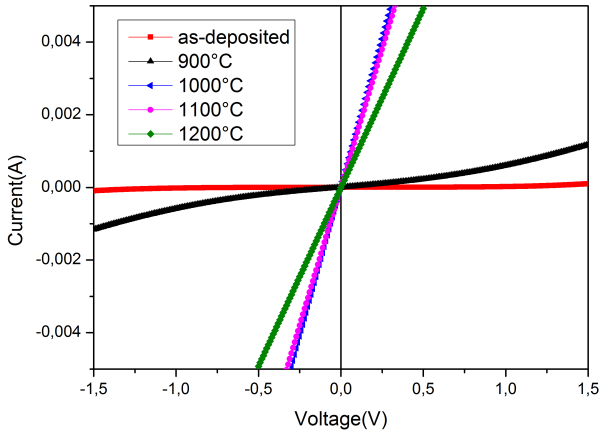

Fig. 2. Current-voltage characteristics measured between 2 adjacent pads of $Ti_{50}Al_{50}$/4H-SiC as-deposited and after annealing at 900, 1000, 1100, 1200°C.

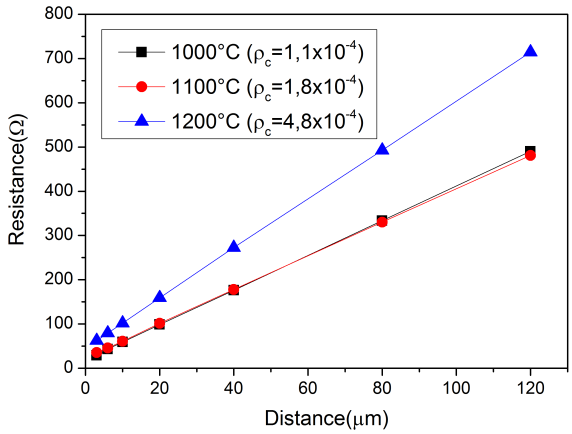

Fig. 3. Variation of the total resistance versus spacing between pads extracted from I-V measurements for $Ti_{50}Al_{50}$/4H-SiC Samples annealed at 1000, 1100 and 1200°C.

TABLE II
SPECIFIC CONTACT RESISTANCE OF ALL SAMPLES AFTER ANNEALING AT VARIOUS TEMPERATURES.

	900°C	1000°C	1100°C	1200°C
$Ti_{20}Al_{80}$	1.1 × 10^{-3} Ω.cm^2	4.1 × 10^{-4} Ω.cm^2	8 × 10^{-4} Ω.cm^2	2 × 10^{-3} Ω.cm^2
$Ti_{30}Al_{70}$	Non-ohmic	2.7 × 10^{-4} Ω.cm^2	3 × 10^{-4} Ω.cm^2	3.4 × 10^{-4} Ω.cm^2
$Ti_{50}Al_{50}$	Non-ohmic	1.1 × 10^{-4} Ω.cm^2	1.8 × 10^{-4} Ω.cm^2	4.8 × 10^{-4} Ω.cm^2
Ti	Non-ohmic	Non-ohmic	Non-ohmic	Non-ohmic

C. Electrical characterization at high temperature

The *I-V* characteristics of $Ti_{50}Al_{50}$, $Ti_{30}Al_{70}$ and $Ti_{20}Al_{80}$ annealed at 1000°C, measured at different temperatures (25, 50, 100, 150, 200, 250, 300, 400, 500, 600°C) display an increase of the current with increasing analysis temperature.

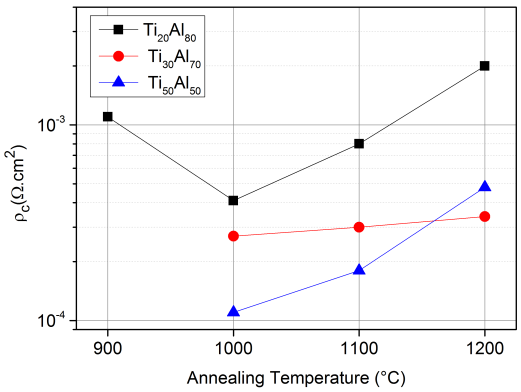

Fig. 4. Evolution of the SCR (ρ_c) measured at room temperature as a function of the annealing temperature of $Ti_{20}Al_{80}$, $Ti_{30}Al_{70}$ and $Ti_{50}Al_{50}$.

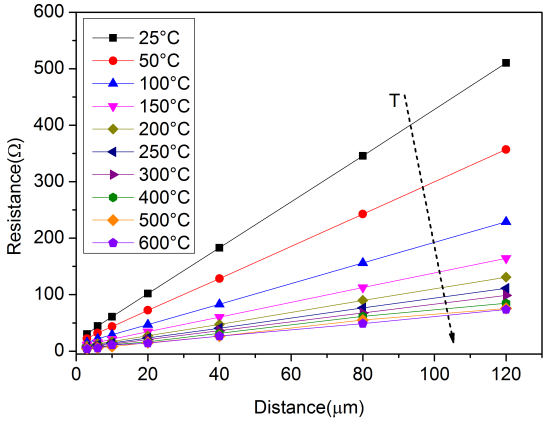

Fig. 5. Variation of the total resistance versus spacing between pads extracted from I-V measurements for $Ti_{50}Al_{50}$/4H-SiC annealed at 1000°C, at different measure temperatures (between 25°C and 600°C).

Fig. 5 shows a typical set of curves obtained from TLM measurements performed at different measurement temperatures (between 25 and 600°C) for $Ti_{50}Al_{50}$/4H-SiC annealed at 1000°C. A similar behavior was observed for $Ti_{30}Al_{70}$/4H-SiC and $Ti_{20}Al_{80}$/4H-SiC annealed at 1000°C. From these curves, we can extract the evolution of the sheet resistance (R_{sh}) of the p-layer (Fig. 6) and the SCR (Fig. 7) as a function of the measurement temperature for each sample. Besides, after these tests were completed and the samples are cooled down to 25°C, R_{sh} and SCR were measured again and it were found not to differ from the values measured before the high temperature tests for each contact type.

For $Ti_{50}Al_{50}$, R_{sh} decreases with increasing measurement temperature, from ~2 kΩ/sq at 300 K to 0.2 kΩ/sq at 875 K. On the other hand, for $Ti_{30}Al_{70}$ and $Ti_{20}Al_{80}$, R_{sh} decreases from ~2.5 kΩ/sq at 300 K to 0.4 kΩ/sq at 875 K, in a similar way.

To determine exactly the doping concentration N_A of the p-layer, the R_{sh} experimental data, reported in Fig. 6, were fitted using the expression of the sheet resistance defined by:

$$R_{sh}(T) = \frac{1}{q\mu_p(T)p(T)e} \quad (1)$$

where "q" is the elementary charge; "$\mu_p(T)$" is the holes mobility, "p(T)" is the free hole concentration and "e" is thickness of the p-layer (in our case t~1.3 μm).

The temperature dependence of the holes mobility $\mu_p(T)$ is giving by the following relation [22]:

$$\mu_p(T) = \mu_p(300)\left(\frac{T}{300}\right)^{-\beta} \quad (2)$$

where "β" is an empirical parameter depending on the doping concentration N_A and "$\mu_p(300)$" is the mobility at 300 K. The values of β and $\mu_p(300)$ results from theoretical calculations (resolution of the electroneutrality equation, calculation of the electron drift mobility as the sum of contribution of the different scattering mechanisms).

The temperature dependence of free hole concentration p(T) is giving by the following relation [23]:

$$\frac{p(T)\times(p(T)+N_D)-n_i^2}{N_A-N_D-p(T)+n_i^2/p} = \frac{N_V}{g}\exp\left(-\frac{E_A}{kT}\right) \quad (3)$$

Where "k" is the Boltzmann constant, "N_D" the concentration of compensating donor, "n_i" the intrinsic carrier

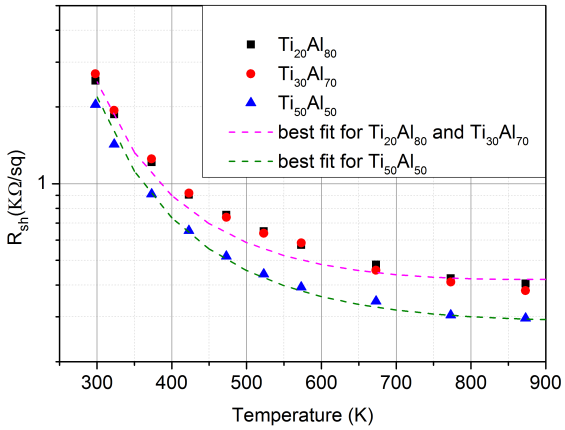

Fig. 6. Temperature dependence of the R_{sh} of the p-layer for $Ti_{20}Al_{80}$, $Ti_{30}Al_{70}$ and $Ti_{50}Al_{50}$ annealed at 1000°C.

density, "N_V" the effective density of states in the valence band, "g" the degeneracy factor for acceptors and "E_A" the ionization energy of acceptors referred to the top of the valence band. This ionization energy is given by [24]:

$$E_A(eV) = 0.265 - 3.6\times10^{-8}\left(1-\frac{N_D}{N_A}\right)^{1/3} N_A^{1/3} \quad (4)$$

Where (N_D/N_A) is the compensation ratio. Note that in equation (3) and (4) N_A and N_D are the total doping concentration and not the ionized dopant concentration (N_A^- and N_D^+).

In these fittings, the doping concentration N_A and the compensation ratio (N_D/N_A) were considered as fitting parameters.

From the best fit in Fig. 6, we found $N_A=1.5\times10^{19}$ cm^{-3} (with 2% compensation, $\mu_p(300)$ = 75 cm^{2}V^{-1}s^{-1} and β = 1.5) for $Ti_{30}Al_{70}$ and $Ti_{20}Al_{80}$ annealed at 1000°C. In the case of $Ti_{50}Al_{50}$ annealed at 1000°C, we found $N_A=3\times10^{19}$cm^{-3} (with 3% compensation, $\mu_p(300)$ = 50 cm^{2}V^{-1}s^{-1} and β = 1.3).

As seen, the N_A value found for $Ti_{50}Al_{50}$ from the temperature dependence fit is higher than those found for $Ti_{20}Al_{80}$ and $Ti_{30}Al_{70}$. This is due to the fact that the doping concentration of the p-layer varies between 1 and 4×10^{19} cm^{-3}. These values of N_A will be used to fit the experimental SCR.

The SCR values of $Ti_{20}Al_{80}$, $Ti_{30}Al_{70}$ and $Ti_{50}Al_{50}$ annealed at 1000°C, as a function of the measuring temperatures, are shown in Fig. 7. As seen, for all cases, with increasing measurement temperatures (between 300 and 875 k) the SCR decreases, from 4.1×10^{-4} to 1.6×10^{-5} Ω.cm² for $Ti_{20}Al_{80}$, from 2.7×10^{-4} to 1.15×10^{-5} Ω.cm² for $Ti_{30}Al_{70}$ and from 1.1×10^{-4} to 9.8×10^{-6} Ω.cm² for $Ti_{50}Al_{50}$. In general, this behavior is due to the increase of Al doping ionization in the p-layer with increasing temperature, a typical behavior of wide band-gap semiconductors with incomplete ionization of the dopants at room temperature [25].

According to the classical theory, there are three transports mechanisms in the metal/semiconductor interface: the thermionic emission (TE), the thermionic field emission (TFE) and the field emission (FE). The ratio kT/E_{00} allowed us to estimate the dominant carrier transport mechanism. E_{00} is a characteristics energy related to the doping density N_A of the p-layer and it can be described by the following relation [26]:

$$E_{00} = \frac{qh}{4\pi}\left(\frac{N_A}{m^*\varepsilon}\right)^{\frac{1}{2}} \quad (5)$$

where "h" is Planck's constant, "m^*" the effective mass of the tunneling hole and ε the dielectric permittivity. in the case of SiC ($\varepsilon = 9.7\varepsilon_0$, ε_0 being the permittivity of free space). In this formula (5) we do not take into account the phenomenon of partial ionization but we used the same value N_A defined as the doping concentration.

For our doping levels and temperature range (300 - 875 k), the ratio kT/E_{00} is found to be ≈ [0.4 – 1.1] for $Ti_{50}Al_{50}$ and ≈ [0.54 – 1.5] for $Ti_{30}Al_{70}$ and $Ti_{20}Al_{70}$. So, TFE can be assumed to be the dominant carrier transport mechanism in the Ti_3SiC_2/SiC interface. Because if $kT/E_{00} \gg 1$ TE is the dominate mechanism, if $kT/E_{00} \ll 1$ FE is the dominate mechanism and if kT/E_{00} is close to 1 TFE is the dominate mechanism.

To determine the Schottky barrier height of the contact, the SCR experimental data, reported in Fig. 7, were fitted using the TFE model. In this model, the SCR can be expressed as [26, 27, 28]:

$$\rho_c = \frac{1}{qA^*}\times\frac{k^2}{\sqrt{\pi\left(\phi_B + V_p\right)E_{00}}}\times cosh\left(\frac{E_{00}}{kT}\right) \times\left[\sqrt{coth\left(\frac{E_{00}}{kT}\right)}\right]\times exp\left(\frac{\phi_B + V_p}{E_0} - \frac{V_p}{kT}\right) \quad (6)$$

Where

$$E_0 = E_{00}coth\left(\frac{E_{00}}{kT}\right) \quad (7)$$

and A* Richardson constant (in the case of SiC, A* = 146 $Acm^{-2}K^{-1}$ [29]) and V_p is the energy difference between the valence-band and the Fermi level.

In these fittings, the Schottky barrier height ϕ_B was considered as fit parameter. The extracted values of ϕ_B from curves in Fig. 7 are reported in Table III. They are found to vary from 0.71 to 0.85 eV. Scorzoni et al. found a value of ϕ_B = 0.82 eV for Ti-Al deposited on p-type ion implanted 4H-SiC

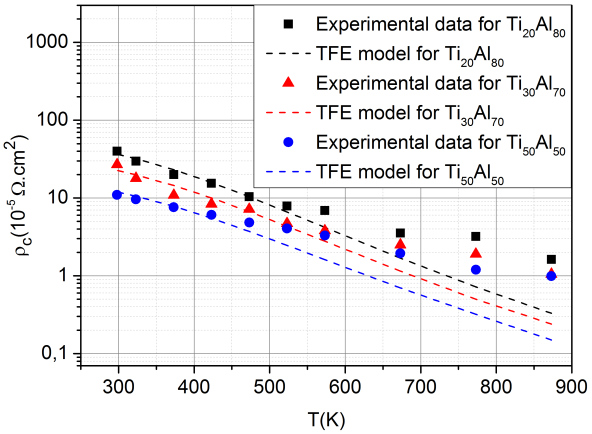

Fig. 7. Temperature dependence of the SCR for $Ti_{20}Al_{80}$, $Ti_{30}Al_{70}$ and $Ti_{50}Al_{50}$ annealed at 1000°C.

[30]. This ϕ_B value is comparable to that found for $Ti_{50}Al_{50}$. On the other hand, a value of ϕ_B = 0.69 eV was fond by Vivona et al. for Ti/Al/W deposited on p-type implanted layer 4H-SiC [31]. This ϕ_B value is close from that found for $Ti_{30}Al_{70}$.

Ageing tests were performed on $Ti_{30}Al_{70}$ at a constant temperature of 600°C in an Ar atmosphere. The contact resistivity was monitored before and after the tests. In fixed time intervals (24, 48, 100, 200 and 400 hours), the contact was cooled down to room temperature, and the contact resistivity was measured. As seen in Fig. 8, the SCR (ρc) has not changed even after 400 hours of aging. So we can deduce that the ohmic contact based on Ti_3SiC_2 is relabel at 600°C even after 400 h of aging.

TABLE III
SCR measured at 25 and 600°C; extracted values of N_A from (R_{sh} – T) characteristics plotted in Fig. 6 and extracted values of ϕ_B from (ρ_c – T) characteristics plotted in Fig. 7.

	N_A (cm^{-3})	SCR at 25°C (Ω.cm²)	SCR at 600°C (Ω.cm²)	ϕ_B (Ev)
$Ti_{20}Al_{80}$	1.5×10^{19}	4.1×10^{-4}	1.6×10^{-5}	0.73
$Ti_{30}Al_{70}$	1.5×10^{19}	2.7×10^{-4}	1.15×10^{-5}	0.71
$Ti_{50}Al_{50}$	3×10^{19}	1.1×10^{-4}	9.8×10^{-6}	0.85

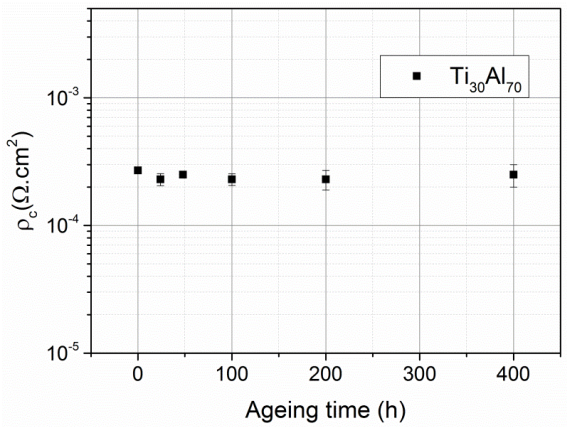

Fig. 8. SCR versus ageing time at 600°C for $Ti_{30}Al_{70}$ annealed at 1000°C.

IV. Conclusion

In this paper, the formation of Ti_3SiC_2 based ohmic contact on 4H-SiC from Ti-Al alloys annealed at high temperature was studied. The role of Ti-Al composition in the initial metallic stacking and the role of the annealing temperature were investigated. XRD analyses show that at very high annealing temperature of Ti-Al, epitaxial Ti_3SiC_2 was replaced by epitaxial TiC. The appearance of TiC at higher annealing temperature seems to be to the detriment of Ti_3SiC_2 while maintaining the epitaxial character. TEM investigation shows that Ti_3SiC_2 cover directly the SiC substrate, this means that Ti_3SiC_2 can be used as an ohmic contact on SiC. For pure Ti annealed at high temperature, Ti_3SiC_2 always co-exists with TiC, but this coexistence was accompanied by some perturbations in the SiC substrate. According to the TLM measurements, all samples annealed at 1000°C (except pure Ti) resulted in the lowest SCR and hence were selected for the high temperature experiments. The temperature dependence of the SCR indicated that TFE is the dominant transport mechanism and the extracted values of ϕ_B vary from 0.71 to 0.85 eV. Finally, when the high temperature tests are completed and the samples are cooled down to 25°C, the SCR were measured again and it were found not to differ from the values measured before the high temperature tests for each contact type. Finally, the ageing tests performed at 600°C under Ar atmosphere showed that Ti_3SiC_2 based contacts were stable and relabel up to 400 h.

References

[1] P. G. Neudeck, D. J. Spry, C. Liang-Yu, G. M. Beheim, R. S. Okojie, C.W. Chang, R. D.Meredith, T. L. Ferrier, L. J. Evans, M. J. Krasowski, and N. F. Prokop, "Stable electrical operation of 6H SiC JFETs and ICs for thousands of hours at 500°C," *IEEE Electron Device Lett.*, vol. 29, no. 5, pp. 456–459, May 2008.

[2] R. S. Okojie, P. Nguyen, V. Nguyen, E. Savrun, D. Lukco, J. Buehler, and T. McCue, "Failure mechanisms in MEMS based silicon carbide high temperature pressure sensors," in *Proc. 45th IEEE Int. Reliab. Phys. Symp.*, 2007, pp. 429–432.

[3] K. Shenai, R.S. Scott, and B.J. Baliga, "Optimum semiconductors for high-power electronics," IEEE Trans. Electron Dev., vol. 36, no. 9, pp. 1811–1823, September 1989.

[4] T.P. Chow, V. Khemka, J. Fedison, N. Ramungal, K. Matocha, Y. Tang, and R.J. Gutmann, "SiC and GaN bipolar power devices," Solid State Electron., vol. 44, no. 2, pp 277–301, February 2000.

[5] F. Roccaforte, A. Frazzetto, G. Greco, F. Giannazzo, P. Fiorenza, R. Lo Nigro, M. Saggio, M. Leszczynski, P. Pristawko, and V. Raineri, "Critical issues for interfaces to p-type SiC and GaN in power devices," Appl. Surf. Sci., vol. 258, no. 21, pp. 8324–8333, August 2012.

[6] Y. Luo, F. Tan, K. Tone, J. Zhao, and J. Crofton, "Searching for device processing compatible ohmic contacts to implanted p-type 4HSiC," Mater. Sci. Forum, 2000, vol. 338-342, pp. 1013–1016.

[7] Z. Wang, S. Tsukimoto, M. Saito, K. Ito, M. Murakami, and Y. Ikuhara, "Ohmic contacts on silicon carbide: The first monolayer and its electronic effect," Phys. Rev. B, vol. 80, no. 24, pp. 245303–12, December 2009.

[8] F. A. Mohammad, Y. Cao, K.C. Chang, and L. M. Porter, "Comparison of Pt-Based Ohmic Contacts with Ti–Al Ohmic Contacts for p-Type SiC," Jpn. J. Appl. Phys., vol.44, no. 8, pp. 5933-5938, April 2005.

[9] R. Konishi, R. Yasukochi, O. Nakatsuka, Y. Koide, M. Moriyama, and M. Murakami, "Development of Ni/Al and Ni/Ti/Al ohmic contact materials for p-type 4H-SiC," Mater. Sci. Eng. B, vol. 98, no.3, pp. 286–293, April 2003.

[10] M.Mysliwiec, M. Sochacki, R. Kisiel, M. Guziewicz, and M. Wzorek, "TiAl–Based Ohmic Contacts on p–Type SiC," in proc. 34th International Spring Seminar on Electronics Technology (ISSE), 2011, pp. 68–72.

[11] N. Thierry-Jebali, A. Vo-Ha, D. Carole, M. Lazar, G. Ferro, D. Planson, A. Henry and P. Brosselard, "Very low specific contact resistance measurements made on a highly p-type doped 4H-SiC layer selectively grown by vapor-liquid-solid transport," Appl. Phys. Lett., vol. 102, no. 21, pp. 212108–**4**, May 2013.

[12] S. Tsukimoto, K. Ito, Z. Wang, M. Saito, Y. Ikuhara, and M. Murakami, "Growth and Microstructure of Epitaxial Ti3SiC2 Contact Layers on SiC," Mater. Trans., vol. 50, no. 5, pp. 1071–1075, March 2009.

[13] K. Buchholt, R. Ghandi, M. Domeij, C. M. Zetterling, J. Lu, P. Eklund, L. Hultman, and A. L. Spetz, "Ohmic contact properties of magnetron sputtered Ti_3SiC_2 on n- and p-type 4H-silicon carbid," Appl. Phys. Lett., vol. 98, no. 4, pp. 042108–3, January 2011.

[14] M.W. Barsoum ,A. Murugaiah ,S.R. Kalidindi, and T. Zhen, "Kinking Nonlinear Elastic Solids, Nanoindentations, and Geology," Phys. Rev. Lett. vol. 92, no. 25, pp. 255508–4, June 2004.

[15] M.W. Barsoum, "The $M_{N+1}AX_N$ phases: A new class of solids: Thermodynamically stable nanolaminates," Progress in Solid State Chem., vol. 28, no. 1, pp. 201–281, 2000.

[16] P. Eklund, M. Beckers, U. Jansson, H. Högberg, and L. Hultman, "The $M_{n+1}AX_n$ phases: Materials science and thin-film processing," Thin Solid Films, vol. 518, no. 8, pp. 1851–1878, August 2010.

[17] M. Utili, M. Agostini, G. Coccoluto, and E. Lorenzini, "Ti_3SiC_2 as a candidate material for lead cooled fast reactor," Nucl. Eng. Des., vol. 241, no. 5, pp. 1295–1300, May 2011.

[18] T. Abi-Tannous, M. Soueidan, G. Ferro, M. Lazar, B. Toury, M.F. Beaufort, J.F. Barbot, J. Penuelas and D. Planson, "Parametric investigation of the formation of epitaxial Ti3SiC2 on 4H-SiC from Al-Ti annealing," Appl. Surf. Sci., vol. 347,pp. 186–192, August 2015.

[19] T. Abi-Tannous, M. Soueidan, G. Ferro, M. Lazar, B. Toury, M.F. Beaufort, J.F. Barbot, J. Penuelas and D. Planson, "A study on the chemistry of epitaxial Ti_3SiC_2 formation on 4H-SiC using Al-Ti annealing," Mater. Sci. Forum, 2015, vol. 821-823, pp. 432–435.

[20] A. Parisini, A. Poggi, and R. Nipoti, "Structural characterization of alloyed Al/Ti and Ti contacts on SiC," Mater. Sci. Forum, 2004, vol. 457-460**,** pp. 837–840.

[21] S. Tsukimoto, K. Ito, Z. Wang, M. Saito, Y. Ikuhara, and M. Murakami, "Growth and microstructure of epitaxial Ti3SiC2 contact layers on SiC," Mater. Trans, vol. 50, no. 5, pp. 1071–1075, March 2009.

[22] H. Matsuura, M. Komeda, S. Kagamihara, H. Iwata, R. Ishihara, T. Hatakeyama, T. Watanabe, K. Kojima, T. Shinohe and K. Arai, "Dependence of acceptor levels and hole mobility on acceptor density and temperature in Al-doped p-type 4H-SiC epilayers," J. Appl. Phys., vol. 96, no. 5, pp. 2708–2715, September 2004.

[23] D.K. Schroder, "Carrier and doping density," in *Semiconductor Material And Device Characterization,* 3rd ed. New York: Wiley.

[24] A. Koizumi, N. Iwamoto, S. Onoda, T. Ohshima, T. Kimoto, K. Uchida and S. Nozaki, "Compensation-Dependent Carrier Transport of Al-Doped p-Type 4H-SiC," Mater. Sci. Forum, 2011, vol. 679-680**,** pp. 201–204.

[25] F. Moscatelli, A. Scorzoni, A. Poggi, G. C. Cardinali, and R. Nipoti, "Improved electrical characterization of Al–Ti ohmic contacts on p-type ion implanted 6H-SiC", Semicond. Sci. Technol, vol. 18, no. 4, pp. 554–559, May 2003.

[26] F. A. Padovani, and R. Stratton, "Field and thermionic-field emission in Schottky barriers," Solid-State Electron., vol. 9, no. 7, pp. 695–707, July 1966.

[27] A. Frazzetto, F. Giannazzo, R. Lo Nigro, V. Raineri and F. Roccaforte, "Structural and transport properties in alloyed Ti/Al Ohmic contacts formed on p-type Al-implanted 4H-SiC annealed at high temperature," J. Phys. D: Appl. Phys., vol. 44, no. 25, pp. 255302–9, June 2011.

[28] A.Y. C.Yu , "Electron tunneling and contact resistance of metal-silicon contact barriers," Solid-State Electron., vol. 13, no.2, pp. 239–247, February 1970.

[29] F. Roccaforte, F. La Via, V. Raineri, R. Pierobon and E. Zanoni, "Richardson's constant in inhomogeneous silicon carbide Schottky contacts," J. Appl. Phys., vol. 93, no. 11, pp. 9137–9144, June 2003.

[30] A. Scorzoni, F. Moscatelli, A. Poggi, G. C. Cardinali and R. Nipoti , "Contact resistivity and barrier height of Al/Ti ohmic contacts on p-type ion implanted 4H- and 6H-SiC," Mater. Sci. Forum, 2004, vol. 457-460, pp. 881–884.

[31] M. Vivona, G. Greco, R. Lo Nigro, C. Bongiorno, and F. Roccaforte, "Ti/Al/W Ohmic contacts to p-type implanted 4H-SiC," J. Appl. Phys., vol. 118, no. 3, pp. 035705–7, July 2015.